Observation of lateral superlattice effects on stepped Cu(001)

X. Y. Wang, X. J. Shen, and R. M. Osgood, Jr.
Columbia Radiation Laboratory, Columbia University, New York, New York 10027

R. Haight and F. J. Himpsel*
T. J. Watson Research Center, IBM Research Division, P.O. Box 218, Yorktown Heights, New York 10598
(Received 3 January 1996)

Lateral superlattice effects are observed for image-state electrons on a stepped Cu(001) surface via angle-resolved two-photon photoemission. Adsorption of Na atoms (~0.01 ML) on the stepped surface enhances the step regularity, yielding clear zone folding with a reduced Brillouin zone given by the reciprocal step lattice. [S0163-1829(96)04323-8]

I. INTRODUCTION

Low-dimensional surface systems have attracted much attention recently because of their fundamental and technological implications. Traditionally, work in these systems has utilized either two-dimensional confinement,[1] viz. the *s-p* surface states on single-crystal copper or that available at heterojunctions in electronic devices,[2] or for lower dimensionality, through lithographic patterning of wires or dots on single-crystal surfaces.[3] Metallic systems with spacer-layer structures have been seen to possess quantum-well states[4] and display effects of oscillatory magnetic coupling,[5] as seen in superlattices with potential applications in magnetic storage.[6] Recently, however, several groups have shown that such low dimensions can be effectively realized and utilized in metals[7–11] via the use of the natural atomic-scale features on vicinally cut surfaces, such as the stepped surfaces created by a small-angle miscut from a low-index plane on a single-crystal metal.[12] Zero-dimensional confinement of electronic states to islands has been observed as well.[13] Electrons affected by these small features have been shown to exhibit a rich variety of standing-wave[9] and scattering[10] phenomena, and lateral confinement of surface electrons.[8,11]

In a recent paper,[8] it was shown that, surprisingly, electrons in image states *just above* the surface of a stepped single-crystal metal exhibited electron localization characteristic of one-dimensional (1D) systems. In this case evidence of an isolated step-induced image state was reported, where the electron movement perpendicular to the steps was believed to be confined by the potential trough at the step edge. It was also suggested that it might be possible for a regular array of step potentials to induce coherent effects for the nearly free electron in movement parallel to the surface. Here we report a direct observation of a surface lateral superlattice on stepped Cu(001) using angle-resolved two-photon photoemission (2PPE). Our results show that the lateral periodicity (~11 Å) of the bare stepped surface leads to backfolding of the dispersion of energy versus parallel momentum $k_{\parallel}$ of the image state. Further, decoration of the step edges with Na atoms sharpens this characteristic dispersive behavior to the point that it can be followed to the edges of the lateral Brillouin zone formed by the step lattice. The reduction of the surface Brillouin zone by a factor of 4.5, compared to that of planar Cu(001), allows a clear observation of backfolding of the free-electron-like dispersion which is normally seen on planar surfaces, yielding an oscillatory dispersive behavior where the electron energy is a multivalued function of $k_{\parallel}$, as seen in the first two Brillouin zones of such a superlattice. Although the effects of the additional reciprocal lattice vector from the step lattice are known in low-energy electron-diffraction (LEED) measurements,[12] they appear to have not been seen previously in the band structure of nanostructured surfaces. The fact that we observe an effect of nanostructuring on the electronic states encourages the development of artificial structures as tailored electronic materials.

II. EXPERIMENT

In the experiment we chose to examine a single-crystal copper surface with a 9.5° miscut to the (001) plane where monatomic steps are formed along the [110] direction. On flat Cu(001) it is well known that a regular progression of stable image states is formed since the vacuum level is coincident with the middle of the projected band gap.[14] Because the energy of the image state is located in the band gap around the $\overline{\Gamma}$ point in the k space for Cu(001), complications due to the interaction of the image-state electron and bulk-state electrons are minimal.

The sample preparation for stepped Cu(001) is similar to that given in Ref. 8. The surface quality was monitored by LEED measurements. The experiments were performed with 17-ns, *p*-polarized laser pulses generated from a three-stage excimer-laser-pumped tunable dye laser. The frequency-doubled laser pulses of photon energies $h\nu = 4.4$–4.6 eV were used to excite the image state on Cu(001); this photon energy range is sufficient to follow the dispersion of energy versus $k_{\parallel}$ over a significant portion ($0 \leqslant |k_{\parallel}| \leqslant 0.35$ Å^{-1}) of the surface Brillouin zone. The data shown here were taken at 4.43 eV. In the angle-resolved experiment, the laser incidence was *fixed* at ~68°, while the detector was rotated within the incidence plane which is perpendicular or parallel to the steps. The details of Na dosing and other aspects in the experiment can be found in Ref. 15. Before making measurements on the stepped surface, a separate planar Cu(001) sample as well as the reverse side of the stepped sample, which was flat (001), were examined via 2PPE and found to

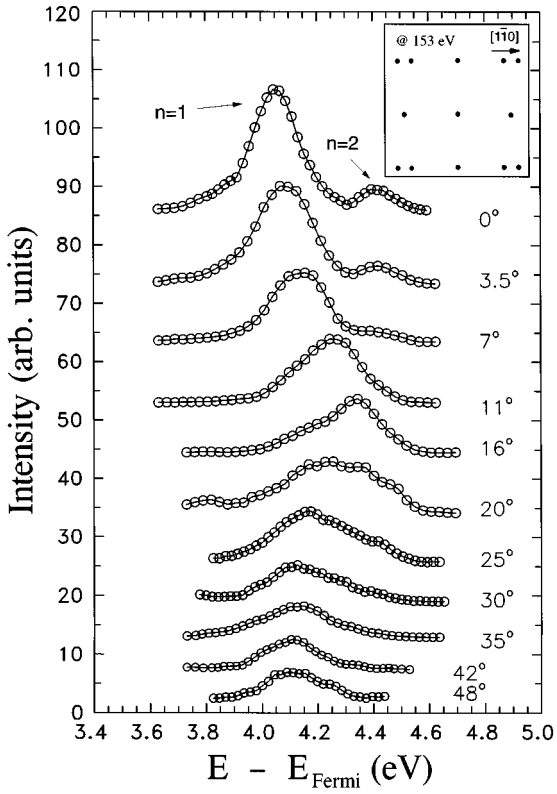

FIG. 1. Angle-resolved two-photon photoemission spectra of image states on stepped Cu(001) in the plane perpendicular to the step edges. The inset shows a schematic diagram of our LEED screen.

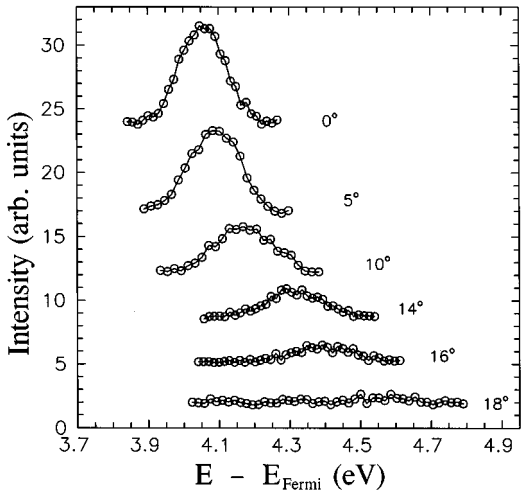

FIG. 2. Angle-resolved two-photon photoemission spectra of the $N=1$ image state on stepped Cu(001) in the plane parallel to the step edges.

display the usual $n=1$ image state with its free-electron-like dispersion.[14]

On the miscut Cu(001), a clear split LEED pattern was observed—indicating its step morphology (see the inset in Fig. 1). However, the somewhat diffuse spots suggested a certain degree of irregularity in step spacing. An analysis[12] of the LEED pattern gave a terrace width of $d=11\pm1$ Å which is in good agreement with the intrinsic terrace width of 4.5 rows of the [110]-oriented atoms for this Cu(119) vicinal surface, $D_0=4.5a/\sqrt{2}=11.5$ Å, where a is the lattice constant of Cu. On this surface, the $n=1$ image state could again be clearly observed; however, its intensity was considerably lower than that for the planar surface. The width of the feature was ~70% larger than that seen on the planar surface, a result which is in accord with a reduced lifetime due to the scattering of image-state electrons from step edges. In addition, observations of the low-energy cutoff of the energy distribution curve (EDC) from 1PPE measurements indicated that the work function on this surface was generally comparable to the 4.63-eV value measured for the planar surface.

III. RESULTS AND DISCUSSION

Angle-resolved photoemission was measured toward the [110] direction (in the plane perpendicular to the steps). The data are shown in Fig. 1 for detection angles θ from 0 to 48°. As a comparison, Fig. 2 shows the data taken in the direction parallel to the steps, where the dispersion is found to be essentially the same as that on the planar surface,[14] i.e., only upwardly dispersive with decreasing signal intensities at larger detection angles until the signal completely disappears (mainly due to the insufficient photon energy of the excitation) at ~18°. The two-photon photoemission in the perpendicular direction also shows (Fig. 1) one feature having parabolic, free-electron-like dispersion up to $\theta\sim16°$. However, in contrast to the dispersion parallel to the steps, the signal on stepped Cu(001) persists throughout the larger detection angles and, more importantly, the dispersion no longer follows a free-electron-like trend. In fact, in this angular region the peak appears to be localized near the bottom of the band at ~4.1 eV above the Fermi level with little dispersion, especially for $\theta\geqslant30°$. Note that our measurements indicated that there was no detectable change in the binding energy of the image state from planar to stepped Cu(001), which was in accord with the work-function measurements mentioned above, since the image states are pinned to the vacuum level.

The addition of even small amounts of alkali-metal atoms to a metal surface is known to affect greatly the local surface potential and structure. On stepped surfaces, alkali adatoms are most likely to adsorb at the step edges,[16] and the resulting strong alkali-induced dipole repulsion would be expected to lead to step repulsion and more regular and stable steps.[12,17] These considerations led us to conduct measurements on a Na-dosed surface. In fact, after low dosage (~0.01 ML) on the stepped Cu(001), the LEED pattern sharpened significantly, i.e., about a factor of 2 reduction in spot width. The split-spot spacing remained the same as before (see the inset in Fig. 3). Adsorption of Na to metal surfaces is also known to alter the work function significantly,[17] e.g., $\Delta\phi=-0.2$ eV for ~0.01 ML. However, since the energies of image states are known to be determined by the *local* work function,[15,18] the energetics of image states on the terraces would not be affected simply on the basis of macroscopic work-function changes—if adsorption occurred mainly at step edges.

Figure 3 shows angle-resolved measurements similar to those shown in Fig. 1 for the surface dosed with ~0.01 ML of Na. Additional data were collected at angular positions

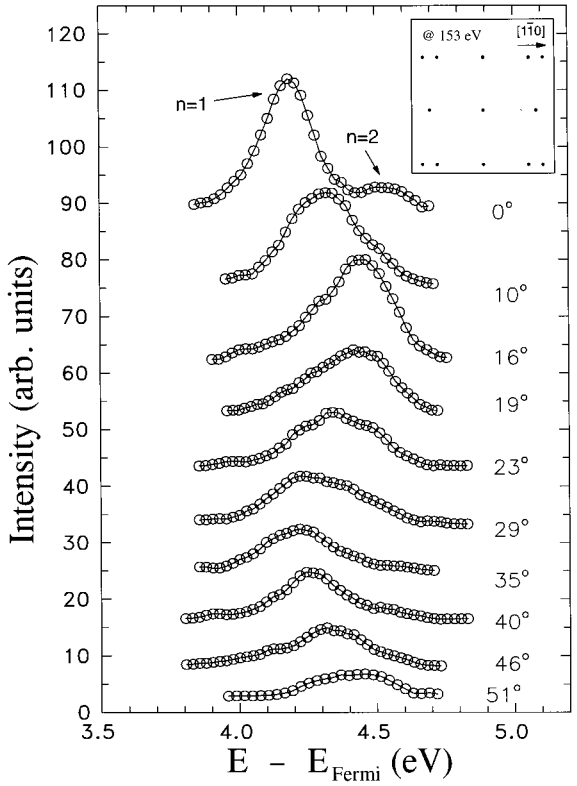

FIG. 3. As Fig. 1, but with a coverage of ~0.01 ML of sodium, which stabilizes an ordered step lattice. The downwards energy dispersion beyond 16° is due to backfolding by the reciprocal step-lattice vector.

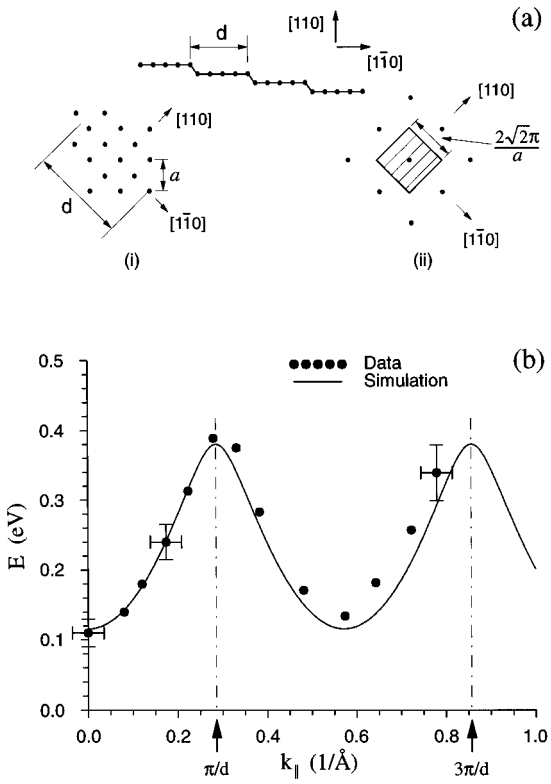

FIG. 4. (a) A sketch of the (i) real-space lattice and (ii) Brillouin zones on stepped Cu(001), where the first Brillouin zone of the planar Cu(001) (bound region) contains 4.5 Brillouin zones of the lateral superlattice in the [110] direction. (b) The dispersion relation of the lateral superlattice formed on Na-decorated, stepped Cu(001). The filled circles are data, the full line is a fit, and the dotted lines indicate the Brillouin-zone boundaries of the step superlattice. The backfolded band between π/d and $3\pi/d$ is absent on the flat Cu(001) surface.

between those displayed, and these data showed same overall angular variation as shown in the figure; for reasons of graphical clarity these were not included in Fig. 3. Note that the image state was of comparable width and signal intensity to those at the bare stepped surface, a result consistent with Na atoms being located at the step edges rather than on terraces. The image-state binding energy was shifted *up* by ~0.12 eV from its value (0.57 eV below the vacuum level) on bare stepped Cu(001), possibly due to confinement to the terrace. More importantly, the dispersive behavior of the surface is greatly improved in clarity; in fact it is clear that backfolding can be seen to occur at $\theta \sim 16°$, followed by an upward dispersion trend starting at $\theta \sim 35°$. Note that repeated experimental measurements showed that the smaller, ''apparent'' multiple peaks seen in some of the data in both Figs. 1 and 3 were simply due to the finite signal-to-noise ratio of the detection system; in other experimental runs these smaller peaks were absent or in other random positions. The broad linewidths seen in some spectra will be addressed below. Because $k_{\parallel}$ is conserved during the photoemission process, one can derive the lateral wave vector of the image-state electron using $k_{\parallel}=(\sqrt{2m_eE_{\rm kin}}/\hbar)\sin\theta$, where $E_{\rm kin}$ is the kinetic energy of the photoemitted electron above the vacuum level. The plot of the transformed data E vs $k_{\parallel}$ is shown as closed circles in Fig. 4(b), where $E=E_{\rm kin}-E_0$ is the electron kinetic energy above the bottom (E_0) of the image-state band of planar Cu(001), as measured from Fig. 3 by peak fitting the data with a standard nonlinear least-square fitting algorithm using a Gaussian line shape. For most of the spectra, only one Gaussian peak was used; for the apparently asymmetrical spectra, the fitting used a dominant Gaussian line shape with a residue Gaussian line shape, and the position of the dominant peak was plotted as closed circles in Fig. 4(b). The backfolding was found to take place at $k_{\parallel}\approx 0.28$ Å^{-1}. The initial dispersion near the zone center can approximately be fitted with a free-electron-like parabolic relation with a ~15% increase in the effective mass ($m^*\approx 1.05m_e$) for the $n=1$ image state, as compared to that of a planar Cu(001), where $m^*=0.9m_e$.[14]

The dispersive behavior displayed in Figs. 3 and 4(b) is in accord with that expected from a lateral surface superlattice, which can be provided by a stepped metal surface with a periodic modulation of the surface potential from the steps. A sketch of the relevant real-space lattice and Brillouin zones on the stepped Cu(001) is shown in Fig. 4(a). For image-state electrons the effective magnitude of the step potential depends on the average distance of the electron from the crystal plane. Electrons in such a 1D periodic potential will display their lateral superlattice nature with the additional Brillouin zone, whose size is determined by the reciprocal step-lattice vector of $g=2\pi/d$. The electrons excited to the image state will experience Bragg reflections, which give rise to zone-folding phenomena, and can be transformed in k space by the step reciprocal-lattice vector **g**, which is 4.5

times smaller than that on the flat Cu(001) as shown in Fig. 4(a). The periodic step potential will result in a multivalued dispersion function which repeats itself beyond $k_{\|}=\pi/d$, *within* the *first* surface Brillouin zone (0–1.23 Å^{-1}) of the flat (001), as seen in Fig. 4(b). In addition, the superlattice potential would also be expected to provide lateral confinement for the image-state electron, leading to a seemingly larger effective mass, as mentioned above.[19]

The differences in the dispersive behavior for the bare and the adsorbate-covered surface can be understood in terms of the behavior of steps on low-index surfaces of noble metals. In particular, steps on Cu(001) are known[20] to exhibit considerable roughness at room temperature (RT) due to fluctuations in the thermal motion of steps on the surface, which accounts for the persistent fuzziness in the LEED pattern of the bare surface. As is apparent from our measurement of a sharper LEED pattern on the dosed surface, Na adatoms stabilize the structure, giving a more regular array of steps and providing a well-defined lateral surface superlattice along the direction perpendicular to the steps. The solid line in Fig. 4(b) shows a typical dispersion relation of the first band obtained from a simple Kronig-Penney model[19] using a square-shaped step potential of width 2.5 Å and height 0.6 V with a period of $d=11$ Å and an effective electron mass $\sim 0.9m_e$. The good agreement between the simulation and experimental data achieved clearly demonstrates the essential effects of zone folding as defined by the lateral superlattice and confinement due to the step potential as well.

Generally, the periodic potential would also give rise to a series of energy bands in the reduced lateral Brillouin zone; the zero-point energy and band gaps of these bands would depend on the strength and detailed structure of the step-edge potential. Based on recent measurements[21] of surface-electron density at step edges, a strongly asymmetric bipolar potential would be reasonable. Test calculations with a Kronig-Penney model shows that such a bipolar potential with appropriately chosen barrier height and well depth can reproduce the binding energy shifts observed on the Na-covered stepped surfaces. Nevertheless, more information on the surface potential at the step sites is needed before our measurement of the change in binding energy can be further assessed.

In another aspect of the experiment, the width of the photoemitted features was seen to depend on whether the detection was toward the [110] or [1$\bar{1}$0] direction (not shown in the figures), i.e., whether the photoemission was uphill or downhill with respect to the steps. In the downhill direction the emitted features were found to be generally broader throughout the angular range, a result which was obtained for a wide range of samples and surface quality. This asymmetric behavior for electrons emitted uphill vs downhill suggests asymmetric scattering at the step edge. This could be caused, for example, by asymmetric interaction with bulk bands: Emission in the uphill direction is closer to the normal of the (001) terraces than in the downhill direction. The interaction with bulk bands is weakest along the [001] direction, where the bulk band gap is widest.[22] Interestingly, such asymmetric behavior is reflected in the data at $\theta>16°$ in Fig. 3. Because of the zone-folding effects, the electrons detected at wave vectors beyond the Brillouin-zone boundary of the superlattice can be viewed as electrons transformed from the first superlattice Brillouin zone by the reciprocal-lattice vector **g**. The peaks in the spectra from 19° to 29° in Fig. 3 are in fact a result of such transformations of the broader peaks for the electrons of $k_{\|}<0$ (i.e., in the downhill direction). In addition, photoemission studies[15,23] have shown that generally the linewidths are narrower for $k_{\|}$ values near the band minimum. Thus, as the detection angle increases further from ~29°, the peaks become sharper, as shown in Fig. 3 because the electrons now come from the bottom of the band and the $k_{\|}>0$ part of the first Brillouin zone, which are of narrower linewidths. As to the broad peak detected at ~51°, the finite angular resolution (~0.05 Å^{-1}) of the detector may have also played a role, because the signal detected at a certain angle may contain contributions from other $k_{\|}$ positions, and the effect of this is especially apparent for detection at the steeper parts of the dispersion parabola [see Fig. 4(b)].

Finally, the fact that the dispersion on the bare stepped surface in Fig. 1 deviates from the ideal is likely due to finite distribution in step spacings for this surface, as reflected in the fuzziness in our LEED pattern and also noted in earlier scanning-tunneling-microscopy (STM) studies.[20] This randomness in the step distribution causes a distribution of backfolding vectors in our photoemission experiment. It is unimportant near the bottom of the band, i.e., at the zone center and at $k_{\|}=2\pi/d$, where the energy is insensitive to $k_{\|}$. However, it becomes substantial at the zone boundaries, where the energy dispersion is strong. The averaging over $k_{\|}$ due to different backfolding vectors washes out the highly dispersive states and leaves only states at the bottom of the band. To investigate this effect quantitatively we used the step width distribution reported for Cu(100) from STM,[20] with each step periodicity creating its own Brillouin zone and consequently its own dispersion. Adding contributions from all the different step periodicities at each detection angle and taking the finite angular resolution of the detector into account, our simulation gives a set of spectra strongly resembling Fig. 1, including the nondispersive feature at the bottom of the band. This feature could be the nondispersive step state seen in Ref. 8. If this is the case, it could be viewed as a state that is localized in the direction perpendicular to the steps by step disorder, in a manner similar to localization phenomena in amorphous semiconductors.[24]

IV. CONCLUSION

In summary, we have observed lateral superlattice effects on a stepped surface, where natural monatomic-height steps are formed with a periodicity of ~11 Å. On surfaces with alkali-atom stabilization of the step edges, the angle-resolved 2PPE data clearly show a reduction of the Brillouin zone from that on the planar surface. This reduction was manifested by the periodic dispersive behavior throughout the first two Brillouin zones for the first band which originated from the $n=1$ image state. One observation, which follows from the band folding and electron confinement, is that the step-edge perturbation in the surface potential is sufficient to form the electronic structure of a lateral superlattice and can

be directly sensed by the image-state electrons despite the fact that these electrons are located a few Å above the Cu surface.[14] The results shown above clearly demonstrate that image-state spectroscopy, in conjunction with angle-resolved 2PPE, provides a unique and sensitive probe of the one-dimensional electronic structure near a stepped surface, and can be readily applied to examine the electronic structure in other low-dimensional systems.

ACKNOWLEDGMENTS

Both R.M.O. and X.Y.W. gratefully acknowledge financial support of this work by the Army Research Office (Contract No. DAAL03-92-G-0191), the Columbia JSEP Program (Contract No. DAAH04-94-G-0057) and the National Science Foundation (Contract No. CTS-94-24252). In addition, R.M.O. would like to thank his son R.M.O. III for drawing his attention to the interest in metal-superlattice structures.

*Present address: Department of Physics, University of Wisconsin at Madison, Madison, WI 53706.

[1] T. Ando, A. B. Fowler, and F. Stern, Rev. Mod. Phys. **54**, 437 (1982).

[2] See, e.g., J. Singh, *Physics of Semiconductors and Their Heterostructures* (McGraw-Hill, New York, 1993).

[3] C. Gourgon, B. Eriksson, L. S. Dang, H. Mariette, and C. Vieu, J. Cryst. Growth **138**, 590 (1994).

[4] J. E. Ortega and F. J. Himpsel, Phys. Rev. Lett. **69**, 844 (1992); J. E. Ortega, F. J. Himpsel, G. J. Mankey, and R. F. Willis, Phys. Rev. B **47**, 1540 (1993).

[5] S. S. P. Parkin, Phys. Rev. Lett. **67**, 3598 (1991).

[6] D. E. Heim, R. E. Fontana, C. Tsang, V. S. Speriosu, B. A. Gurney, and M. L. Williams, IEEE Trans. Mag. **30**, 316 (1994).

[7] J. E. Ortega and F. J. Himpsel, Appl. Phys. Lett. **64**, 121 (1994); F. J. Himpsel, Y. W. Mo, T. Jung, J. E. Ortega, G. J. Mankey, and R. F. Willis, Superlatt. Microstruct. **15**, 237 (1994).

[8] J. E. Ortega, F. J. Himpsel, R. Haight, and D. R. Peale, Phys. Rev. B **49**, 13 859 (1994).

[9] Y. Hasegawa and Ph. Avouris, Phys. Rev. Lett. **71**, 1071 (1993); M. F. Crommie, C. P. Lutz, and D. M. Eigler, Nature **363**, 524 (1993).

[10] R. S. Williams, P. S. Wehner, S. D. Kevan, R. F. Davis, and D. A. Shirley, Phys. Rev. Lett. **41**, 323 (1978); A. P. Shapiro, T. Miller, and T.-C. Chiang, Phys. Rev. B **38**, 1779 (1988).

[11] O. Sanchez, J. M. Garcia, P. Segovia, J. Alvarez, A. I. Vazquez de Parga, J. E. Ortega, M. Prietsch, and R. Miranda, Phys. Rev. B **52**, 7894 (1995).

[12] H. Wagner, in *Solid State Physics*, edited by J. Holzl, F. K. Schulte, and H. Wagner, Springer Tracts in Modern Physics Vol. 85 (Springer, New York, 1979), pp. 151–221.

[13] R. Fischer, Th. Fauster, and W. Steinmann, Phys. Rev. B **48**, 15 496 (1993).

[14] K. Giesen, F. Hage, F. J. Himpsel, H. J. Riess, and W. Steinmann, Phys. Rev. B **35**, 971 (1987); K. Giesen, F. Hage, F. J. Himpsel, H. J. Riess, W. Steinmann, and N. V. Smith, *ibid.* **35**, 975 (1987).

[15] X. Y. Wang, R. Paiella, and R. M. Osgood, Jr., Phys. Rev. B **51**, 17 035 (1995).

[16] E. V. Albano and H. O. Martin, Phys. Rev. B **38**, 7932 (1988); S. Kennou, M. Kamaratos, S. Ladas, and C. A. Papageorgopoulos, Surf. Sci. **216**, 462 (1989).

[17] *Physics and Chemistry of Alkali Metal Adsorption*, edited by H. P. Bonzel, A. M. Bradshaw, and G. Ertl (Elsevier, Amsterdam, 1989); T. Aruga, H. Tochihara, and Y. Murata, Phys. Rev. B. **34**, 8237 (1986); N. C. Bartelt, T. L. Einstein, and E. D. Williams, Surf. Sci. Lett. **240**, L591 (1990); C. Jayaprakash, C. Rottman, and W. F. Saam, Phys. Rev. B **30**, 6549 (1984).

[18] R. Fischer, S. Schuppler, N. Fisher, Th. Fauster, and W. Steinmann, Phys. Rev. Lett. **70**, 654 (1993).

[19] H. M. Rosenberg, *The Solid State* (Oxford University Press, New York, 1988).

[20] J. Frohn, M. Giesen, M. Poensgen, J. F. Wolf, and H. Ibach, Phys. Rev. Lett. **67**, 3543 (1991); M. Poensgen, J. F. Wolf, J. Frohn, M. Giesen, and H. Ibach, Surf. Sci. **274**, 430 (1992).

[21] Ph. Avouris, I.-W. Lyo, and P. Molinas-Mata (unpublished).

[22] We are indebted to Steven D. Kevan for suggesting this explanation.

[23] S. D. Kevan, Phys. Rev. Lett. **50**, 526 (1983); J. Tersoff and S. D. Kevan, Phys. Rev. B **28**, 4267 (1983); S. D. Kevan, *ibid*. **33**, 4364 (1986).

[24] P. W. Anderson, Phys. Rev. **109**, 1492 (1958).